IJCRT.ORG ISSN : 2320-2882

INTERNATIONAL JOURNAL OF CREATIVE RESEARCH THOUGHTS (IJCRT)

An International Open Access, Peer-reviewed, Refereed Journal

Investigating The Optoelectronic Behaviour Of Non-Covalently Functionalized Graphyne With Aniline Yellow (Cis/ Trans) Through DFT Calculations And MD Simulations

Bachan Meena*

Assistant Professor, Department of Chemistry, Atma Ram Sanatan Dharma College, University of Delhi, New Delhi, India

Abstract

Context

Recent years have seen a significant increase in interest in the photochemistry of the azo (-N=N-) group due to its photodynamic features associated with the reversible trans-cis-trans isomerization cycle. The research investigates the effect of different substituents on aniline yellow dye in trans and cis forms. The best derivatives (AYC1/AYT1) are further explored with a graphyne sheet. The research gives valuable results and might be useful for photoswitching molecules.

Method

The structural, and electronic properties and UV-Vis absorption behavior of derivatives were examined by the computational analysis such as Density Functional theory (DFT), time-dependent DFT (Gaussian), and density of states (DOS). Additionally, utilizing molecular dynamics (MD) simulations (GROMACS) to explore the interactions between the graphyne and the isomers (E and Z) of aniline yellow.

Keywords: Density functional theory, Azo compounds, Aniline yellow, Photoswitching, Molecular dynamics

Graphical Abstract:

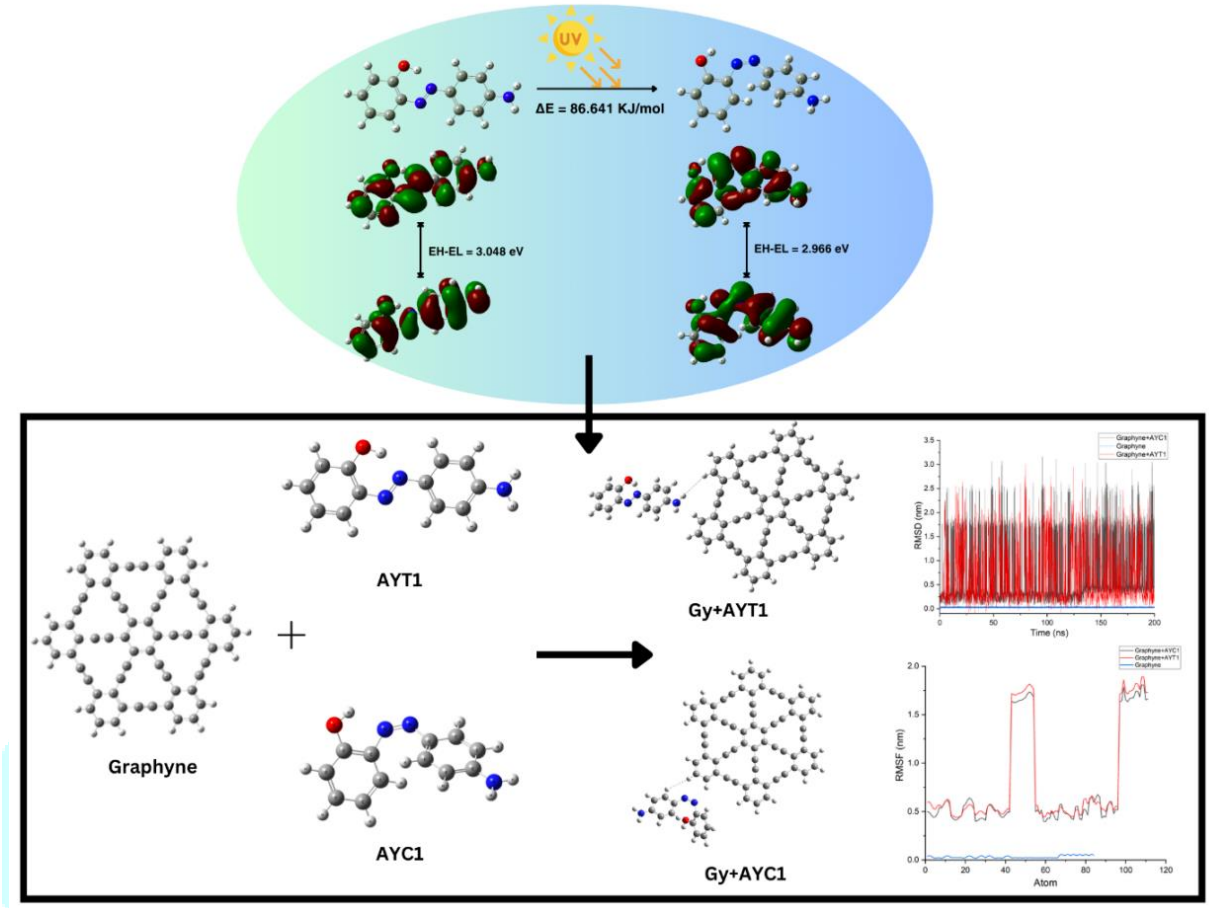

Introduction

Azo-containing molecules obtained significant attention in the field of photoswitches because of their versatile nature and the potential to undergo reversible structural changes in response to light [1]. This category of compounds, a key component of the synthetic organic chemical field, exhibits fascinating biological activities and is widely used as indicators for different titrations in analytical chemistry as well as used in the dye industry. Apart from their biological and dyeing characteristics, azo compounds show unique geometrical and electrical properties that make them suitable candidates for reversible optical data storage [2],[3].

The Azo unit (-N=N-) is attributed to its fascinating properties, including narrow bandgap, lewis's base characteristic, and redox activity. The existence of delocalized Π-electrons and a centered π-π* transition at the azo chromophore gives even more attraction towards it [4]. The Azo moiety exhibits special cis-trans isomerization properties when exposed to UV light [5] causing a significant shift in geometry and movement of molecules during photoisomerization. This characteristic makes azo compounds desirable components for creating light-driven molecular electronics [6].

Molecular photoswitching is an attractive phenomenon in several fields of study, such as photopharmacology, biology, data storage, and solar energy storage [7]. Photoswitching involves molecules that can reversibly switch between (at least) two states cis and trans when exposed to light. The integration of photoswitches into multifunctional systems is highly relevant to the development of next-generation

materials [8]. Among different categories of photochromic molecules, azobenzene stands out as the most widely used photoswitches because of their reliability, stability, and tunability. Low-intensity light circumstances allow steady switching between Z and E isomers due to azobenzene's strong quantum yields and extinction coefficients [9], [10].

Photoisomerization trans-cis-trans cycle is the main property of the chromophore group, which is widely used in reversible optical storage, non-linear optical components, light-driven optical switches, and other photonics applications. Since the cis (Z) twist conformation has more energy due to the orbitals' repulsion between the aromatic ring and prohibited orbital symmetry, the trans isomer is more stable thermodynamically than the cis isomer [11], [12].

Carbon based allotropes hold fascinating but uniquely different chemical and physical characteristics [13]. Graphyne (Gy) are considerably more important because of their distinct structural and electrical characteristics. Graphyne exhibits several distinct chemical, electrical, mechanical, and structural characteristics with significant applications in nanoelectronics and energy storage [14]. These substances are seen to be fascinating possibilities for applications in energy storage, desalination, electrical devices, and hydrogen purification, among other areas. since they contain carbon having sp and sp^2 hybridization [15]. Hence, graphyne alters with photochromic molecules that might modify their energy storage properties.

In recent decades, quantum chemistry methodologies have been applied to better comprehend the link between dye characteristics and its molecular geometries. Providing a solid theoretical foundation for the fast screening of effective dyes [16]. Density functional theory (DFT) is one of the essential and useful techniques used to describe the chemical and electrical structure of the compound and provide more accurate and precise results than other methods [17]. TD-DFT based computations are increasingly being used to characterize the behavior of FMOs that participate in the transitions of electrons and the electronic structure in the excited state [18]. Molecular dynamics simulations determine the complex's structural stability [19].

In this work, the aniline yellow dye is investigated, and comes under the category of azo dye, using density functional theory calculations. The goal is to investigate how substituents or other functional groups and the presence of graphyne affect the molecular structure of these dyes, using DFT calculations to anticipate stable structures for both E and Z isomers. In addition, we used time-dependent DFT (TD-DFT) to investigate the UV-Visible absorption behavior of derivatives. Furthermore, the binding features or interactions between the isomers of aniline yellow with graphyne and the stability of molecules were further investigated using molecular dynamics (MD) simulation techniques. These comprehensive methods allow us to understand and tune the characteristics of azo containing molecules for improved photoswitching molecules.

Table 1: Different substituent groups and their position on cis/trans isomer of aniline yellow.

S.no.	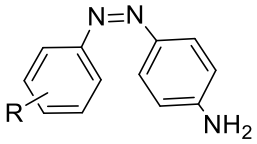		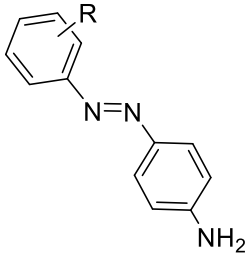	
	Cis		Trans	
	R	CMPD. number	R	CMPD. number
1	2-OH	AYC1	2-OH	AYT1
2	2-Cl	AYC2	2-Cl	AYT2
3	2-CH_3	AYC3	2-CH_3	AYT3
4	2-OCH_3	AYC4	2-OCH_3	AYT4
5	2-COOH	AYC5	2-COOH	AYT5
6	3-OH	AYC6	3-OH	AYT6
7	3-Cl	AYC7	3-Cl	AYT7
8	3-CH_3	AYC8	3-CH_3	AYT8
9	3-OCH_3	AYC9	3-OCH_3	AYT9
10	3-COOH	AYC10	3-COOH	AYT10

Computational calculations

Density functional theory (DFT) calculations

The chemical structure of aniline yellow and its derivatives was drawn by ChemDraw Professional 15.0 (Table 1) [20]. The GAUSSIAN software was utilized to optimize the electronic structure and molecular geometry of the molecules under study [21], [22]. We have looked at the trans and cis forms of every molecule under consideration, as well as the locations of the functional groups inside the molecule. The calculations are performed out using DFT at b3lyp/6-311g basis set for aniline yellow and derivatives but for graphyne with aniline yellow derivative uses b3lyp/3-21g basis set [23], [24]. TD-DFT calculations were carried out of Z and E isomers of the derivatives of aniline yellow after the optimization of geometry at b3lyp/6-311g basis set [11]. The density of states (DOS) analysis of graphyne, graphyne+AYC1 (Gy+AYC1), and graphyne+AYT1 (Gy+AYT1) complexes was carried out using GaussSum [25].

Molecular dynamics (MD) simulations

MD simulations were carried out to investigate the interactions between the graphyne and aniline yellow derivatives and the stability of complexes. The topology file of graphyne, Gy+AYC1, and Gy+AYT1 complexes was prepared by using Swiss Param [26]. MD simulations were performed using GROMACS over a period of 200 nanoseconds and CHARMM27 force field was applied for MD simulation. MD simulations provide different trajectories, such as root mean square fluctuations (RMSF) and root mean square derivatives (RMSD) which state the stability of the complexes [27]. The structures were minimized

and then brought to equilibrium. The equilibration occurred in an isothermal-isochoric ensemble, and NVT, which stands for a constant number of particles, volume, and temperature, at 300K for 100 ps. In an isothermal-isobaric NPT (constant number of particles, pressure, temperature) ensemble, the second stage of equilibration was conducted at 300 K and 1 bar of pressure for 100 ps. Next, the computations were run in water for 200 ns [28].

Results and discussion

Frontier molecular orbitals

DFT computations were used to examine the electronic properties of aniline yellow dye. The method included the determination of the frontier molecular orbitals (FMO) (lowest unoccupied molecular orbitals (LUMO) and highest occupied molecular orbitals (HOMO)), dipole moment, optimization energy, and optimized geometry. The HOMO, LUMO, and optimized geometry of aniline yellow are shown in Figure 1 and Figure S1 of supplementary file [29].

The LUMO functions as an electron acceptor, whereas the HOMO exhibits the capacity to donate an electron [30]. The E_{HOMO}-E_{LUMO} plays an important factor in explaining the movement of charge within the molecule [31] and also identifying a compound's kinetic stability, chemical reactivity, electrical properties, and optical polarizability [2]. Higher energy gap values are associated with higher compound stability [30], lower electrical conductivity, and higher kinetic stability with lower chemical reactivity due to the increase in the potential of charge transfer, charge transfers are also accountable for the molecule's NLO reaction [32], [33], [34]. The lower E_{HOMO}-E_{LUMO} value also shows a better potential for donating electrons and an improved nonlinear optical response of the compounds [35]. Soft molecules generally have a small energy gap and will be more polarizable than hard molecules [36]. Dipole moment analyses were carried out to assess the polarity of the molecule where the NLO features exhibited higher activity [30].

The photochromic behavior of molecules is determined by the energy difference between their E and Z isomers. A higher energy difference between the Z and E isomers is required to achieve effective photochromism [37]. The calculated results of the change in energy of the parent molecule and its derivatives are summarized in Table 2 and E_{HOMO} and E_{LUMO} are shown in Table 3. The change in energy between the cis and trans isomer of the parent molecule (AYC and AYT) is 63.012 KJ/mol, which is less than its two derivatives AYC1/AYT1 and AYC6/AYT6 which is 86.641 and 65.637 KJ/mol respectively. The change in energy of AYC1/AYT1 is found to be maximum. The first derivative produced the most useful outcomes out of all the derivatives [37]. Additionally, the result of $E_{HOMO} - E_{LUMO}$ gap in eV of AYC1 and AYT1 (2.966 and 3.048 respectively) is lesser than parent molecules AYC and AYT (3.374 and 3.238 respectively). A lower E_{HOMO}-E_{LUMO} gap gives higher chemical reactivity, electrical conductivity [32], [38], and better potential for electron donation nonlinear property [35]. Hence, results show that these derivatives have the potential and might be used as photoswitching molecules.

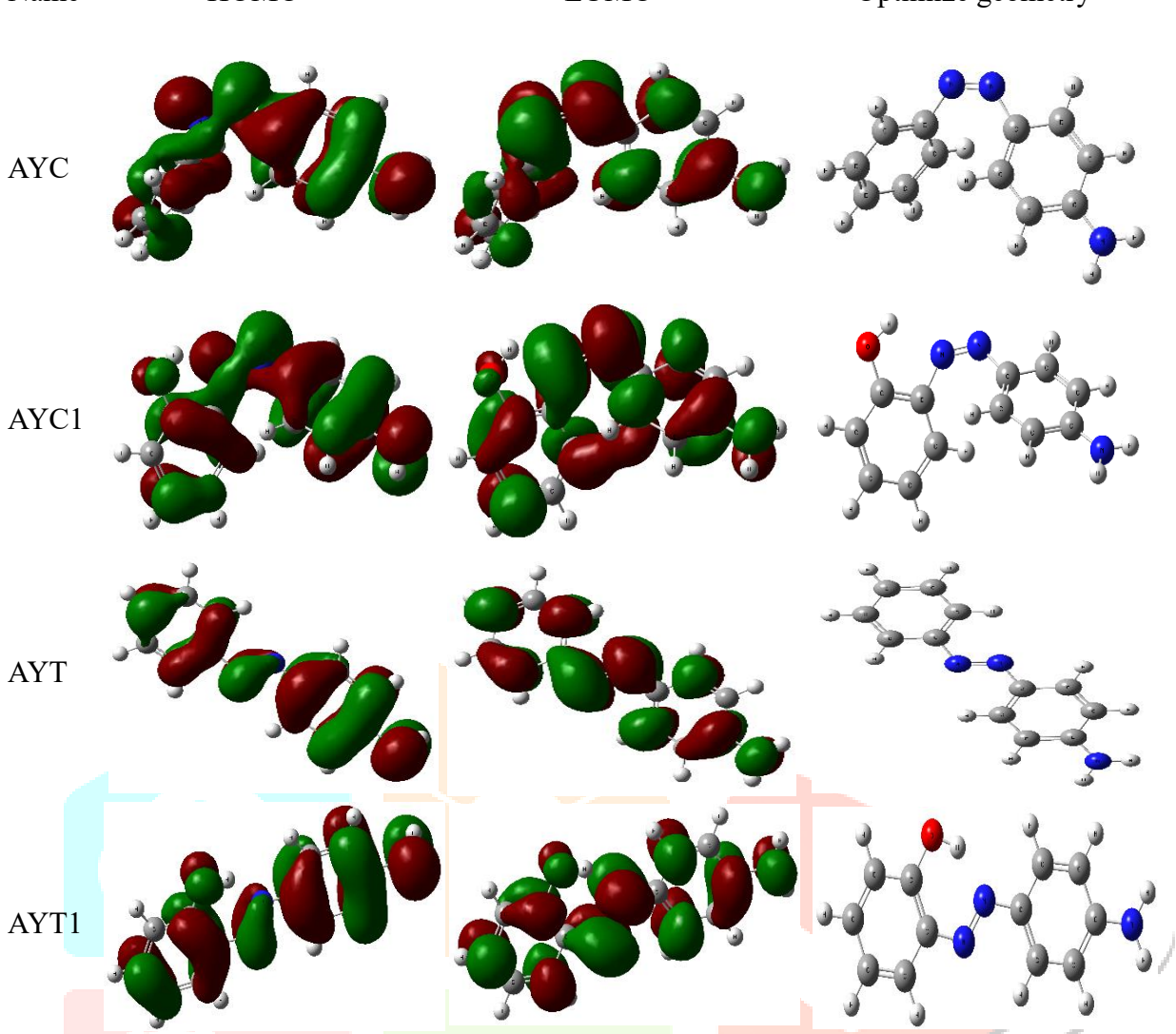

Figure 1: Visual illustrations of optimized geometry, HOMO, and LUMO of cis and trans isomers of aniline yellow.

Table 2: Calculated optimization energy, dipole moment, and change in energy of aniline yellow and derivatives.

Cis		Trans				
Name	Optimization energy (Hartree)	Name	Optimization energy (Hartree)	Change in energy (Hartree per particle)	Change in energy (kJ/mol)	Change in energy (eV)
AYC	-628.083	AYT	-628.107	0.024	63.012	0.653
AYC1	-703.305	AYT1	-703.338	0.033	86.641	0.898
AYC2	-1087.687	AYT2	-1087.700	0.013	34.131	0.354
AYC3	-667.399	AYT3	-667.418	0.019	49.884	0.517
AYC4	-742.594	AYT4	-742.601	0.007	18.378	0.190
AYC5	-816.640	AYT5	-816.664	0.024	63.012	0.653

AYC6	-703.302	AYT6	-703.327	0.025	65.637	0.680
AYC7	-1087.688	AYT7	-1087.710	0.022	57.761	0.599
AYC8	-667.399	AYT8	-667.423	0.024	63.012	0.653
AYC9	-742.600	AYT9	-742.624	0.024	63.012	0.653
AYC10	-816.649	AYT10	-816.667	0.018	47.259	0.489

Table 3: Calculated E_{HOMO}, E_{LUMO}, E_{HOMO}-E_{LUMOse} of aniline yellow and derivatives.

Cis					Trans				
Name	E_{HOMO}	E_{LUMO}	E_{HOMO}-E_{LUMO} (Hartree per particle)	E_{HOMO}-E_{LUMO} (eV)	Name	E_{HOMO}	E_{LUMO}	E_{HOMO}-E_{LUMO} (Hartree per particle)	E_{HOMO}-E_{LUMO} (eV)
AYC	-0.206	-0.082	0.124	3.374	AYT	-0.208	-0.089	0.119	3.238
AYC1	-0.202	-0.093	0.109	2.966	AYT1	-0.207	-0.095	0.112	3.048
AYC2	-0.213	-0.087	0.126	3.428	AYT2	-0.212	-0.091	0.121	3.292
AYC3	-0.205	-0.081	0.124	3.374	AYT3	-0.206	-0.085	0.121	3.292
AYC4	-0.206	-0.086	0.12	3.265	AYT4	-0.215	-0.091	0.124	3.374
AYC5	-0.212	-0.087	0.125	3.401	AYT5	-0.213	-0.095	0.118	3.211
AYC6	-0.207	-0.083	0.124	3.374	AYT6	-0.208	-0.091	0.117	3.184
AYC7	-0.211	-0.087	0.124	3.374	AYT7	-0.212	-0.096	0.116	3.156
AYC8	-0.205	-0.082	0.123	3.347	AYT8	-0.207	-0.089	0.118	3.211
AYC9	-0.207	-0.082	0.125	3.401	AYT9	-0.208	-0.090	0.118	3.211
AYC10	-0.209	-0.087	0.122	3.320	AYT10	-0.212	-0.096	0.116	3.156

UV spectra analysis

The UV-Visible spectra of E and Z isomers of derivatives of aniline yellow were obtained using time dependent DFT (TD-DFT) [39], displayed in Figure 2 and S2, and the maximum absorption wavelength is summarized in **Table 4**. A shift in the absorption band intensity enables the monitoring of cis-trans-cis isomerization. The band associated with the π-π* transition moves toward shorter waves upon conversion to the cis-isomer, whereas the n-π* transition takes place at a higher wavelength [40], [41]. Spectra were computed using Origin to determine the band locations [42]. A noticeable decrease was observed in the wavelength of the parent molecule moving from trans (AYT) to cis (AYC) isomer. Similarly seen in moving from AYT1 to AYC1 (Figure 2), Thus, these are associated with the π-π* transition. In some of the derivatives observed the wavelength increases (redshift) as well as decreases (blueshift), hence these are

associated with both n-π* and π-π* transitions respectively (Table 4 and Figure S2 of supplementary file). The derivatives in the trans state show absorption bands from 340-670 nm and in the cis state from 345 to 550 nm (**Table 4**).

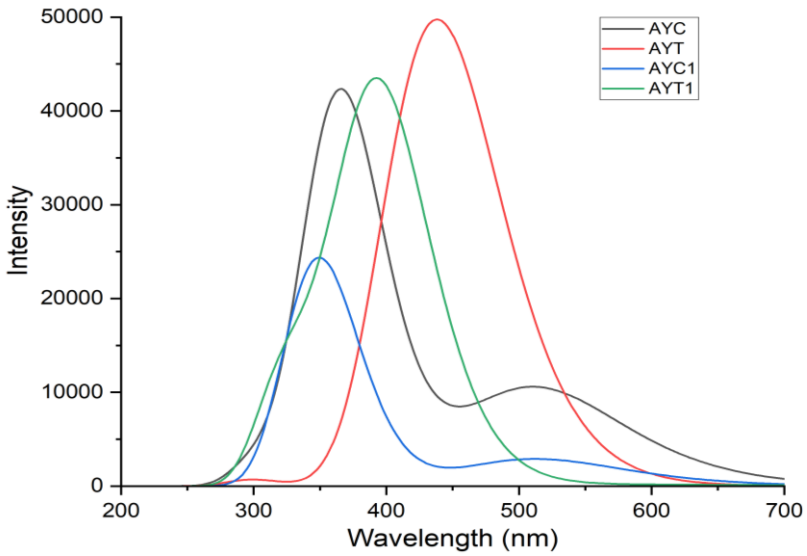

Figure 2: UV-visible spectra of aniline yellow and derivative.

Table 4: Maximum absorption wavelength (λ_{max}) of aniline yellow and derivatives.

Name	λ_{max} (nm)	Name	λ_{max} (nm)
AYC	366.4	AYT	438.4
AYC1	349.2	AYT1	392.8
AYC2	394.2	AYT2	416.0
AYC3	376.2	AYT3	347.2
AYC4	360.0	AYT4	423.0
AYC5	480.0	AYT5	664.0
AYC6	352.8	AYT6	362.0
AYC7	459.0	AYT7	366.4
AYC8	361.8	AYT8	359.8
AYC9	466.0	AYT9	362.0
AYC10	542.4	AYT10	370.8

DFT calculations of graphyne with AYC1/AYT1

The change in energy between Gy+AYC1 and Gy+AYT1 is much higher than between AYC1 and AYT1 102.394 and 86.641 kJ/mol respectively. (**Table 5**) A higher energy difference between the Z and E isomers is required to achieve effective photochromism [37]. This states that graphyne with an aniline yellow derivative might be good for photoswitching or energy storage. The interactions between the graphyne with AYC1 and AYT1 are studied. The interactions are visible in the optimized geometry shown

in Figure 3. In Gy+AYC1, the hydrogen atom of the graphyne sheet interacts with the hydrogen atom of the aniline yellow derivative, and the bond length is 2.926A°. In Gy+AYT1, the hydrogen atom of the graphyne sheet interacts with an amine group of aniline yellow derivative and forms a bond of bond length 3.057A°.

The derivatives such as AYC1 and AYT1 which give valuable outcomes are further explored. Graphyne (Gy) interacts with AYC1 and AYT1 to investigate the effect of graphyne on the properties of the aniline yellow derivative. The optimized geometry, HOMO, and LUMO are given in Figure 3. Higher HOMO energy (E_{HOMO}) values give rise to nucleophilicity, while lower LUMO energy (E_{LUMO}) molecules are more likely to undergo electron transfer and exhibit higher electrophilicity [43]. In Gy+AYC1, the HOMO electron density extended towards the AYC1 molecule. Although the electron density of LUMO delocalized around the center carbon chain of graphyne. In Gy+AYT1, the HOMO electron density extended towards the AYT1 molecule. While the electron density of LUMO delocalized around the center carbon chain of graphyne. The E_{HOMO}-E_{LUMO} of Gy+AYC1 and Gy+AYT1 is 2.231 and 2.286 eV respectively is lesser than AYC1 and AYT1 (**Table 6**). Hence, after the addition of graphyne in aniline yellow derivatives the E_{HOMO}-E_{LUMO} gap was reduced. This states that Gy+AYC1 and Gy+AYT1 are more chemically reactive, more electrically conductive, less kinetic stable, and have a better potential for electron donation nonlinear properties than AYC1 and AYT1 respectively [30], [33], [35]. s

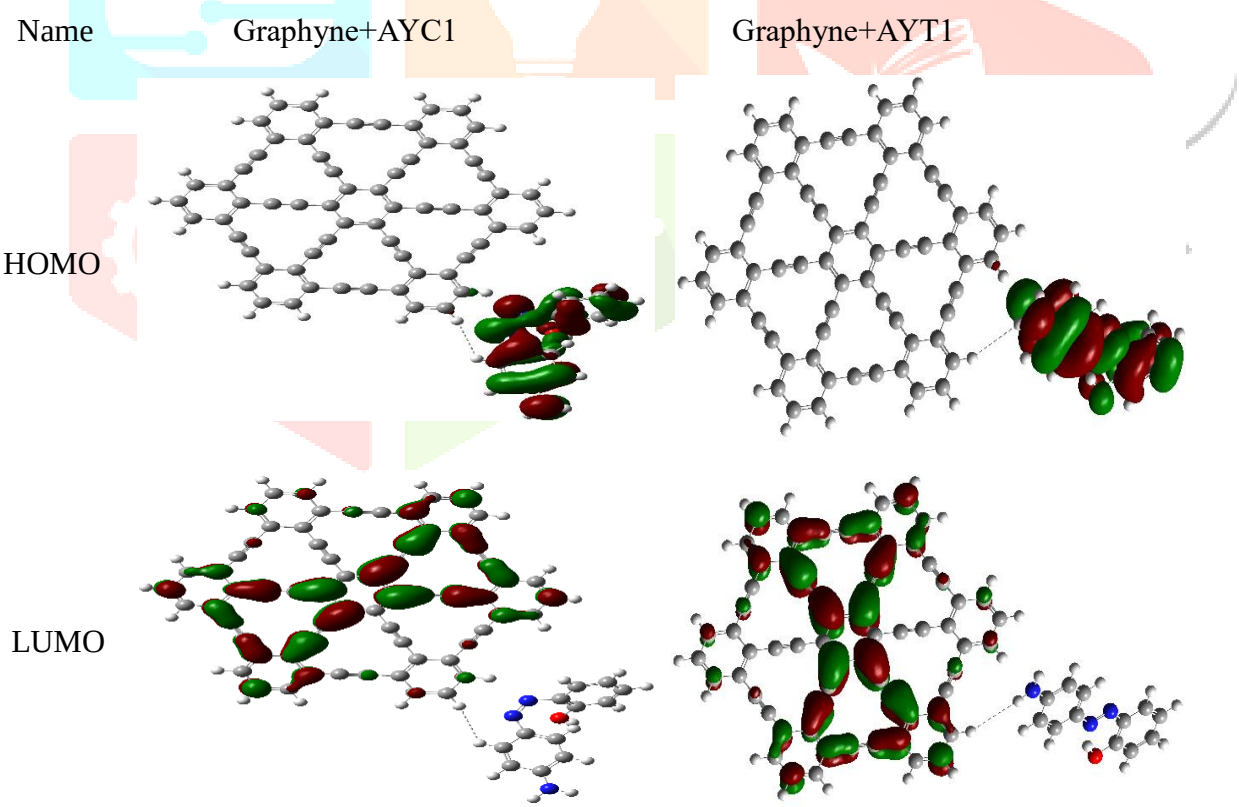

Optimize geometry

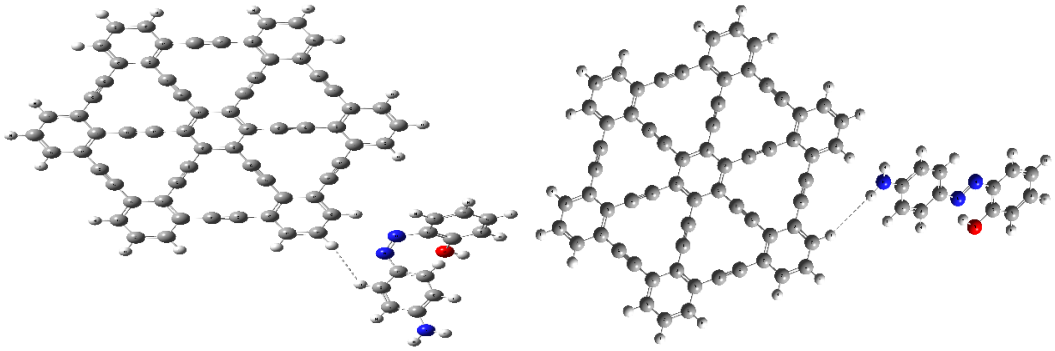

Figure 3: visual illustrations of optimized geometry, HOMO, and LUMO of graphyne with AYC1 and AYT1.

Table 5: Calculated optimization energy, dipole moment, and change in energy of graphyne with AYC1 and AYT1.

Cis			Trans					
Name	Optimization energy (Hartree)	Dipole moment (Debye)	Name	Optimization energy (Hartree)	Dipole moment (Debye)	Change in energy (Hartree per particle)	Change in energy (kJ/mol)	Change in energy (eV)
Gy+AYC1	-3210.814	12.351	Gy+AYT1	-3210.853	6.882	0.039	102.394	1.061

Table 6: Calculated E_{HOMO}, E_{LUMO}, E_{HOMO}-E_{LUMO} of graphyne with AYC1 and AYT1.

Name	E_{HOMO}	E_{LUMO}	E_{HOMO}-E_{LUMO} (Hartree per particle)	E_{HOMO}-E_{LUMO} (eV)
Gy+AYC1	-0.197	-0.115	0.082	2.231
Gy+AYT1	-0.199	-0.115	0.084	2.286

Density of states (DOS) spectra analysis

The DOS analysis of graphyne, Gy+AYC1, and Gy+AYT1 complexes was carried out using GaussSum [25], using DFT calculations (Figure 4). The charge transfer and electronic structure between the complexes' active sites of the complexes can be predicted using the information obtained from DOS spectra, which reveal the number of states accessible at each energy level. The locations of the peaks in the DOS spectra indicate the electronic energy levels present in the molecule. The probability of charge transfer within the complex increases with decreasing band gap [44], [45]. There was observed a bandgap of -1.873eV in the graphyne. A drop in the bandgap to −1.423 and -1.498eV was seen in the Gy+AYC1 and Gy+AYT1 complexes respectively, suggesting a greater probability of charge transfer, which is also

observed in the E_{HOMO}-E_{LUMO} gap by DFT calculation. The DOS's sharp peaks signify a stronger interaction between the graphyne and derivatives due to a higher intensity of charge transfer.

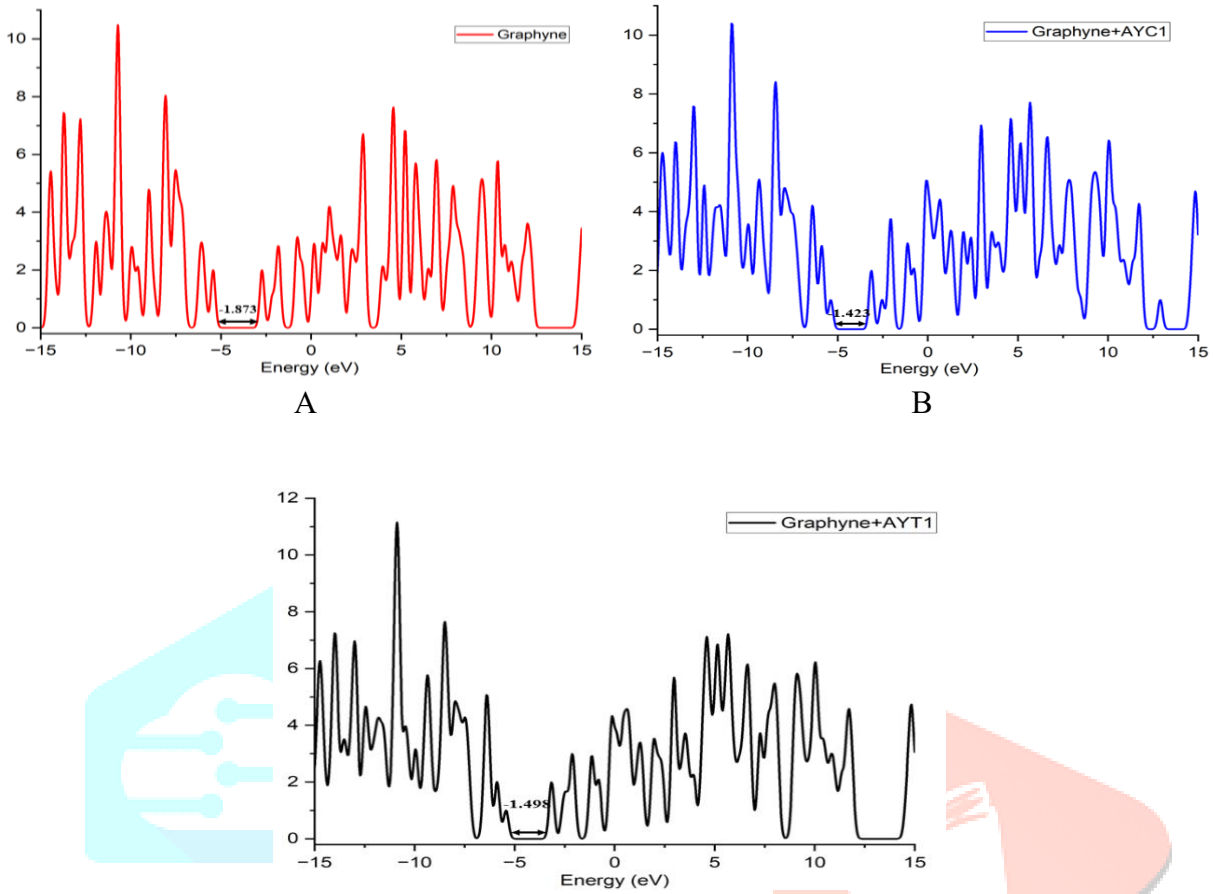

Figure 4: The density of states (DOS) spectra of (A) graphyne, (B) Gy+AYC1, and (C) Gy+AYT1 complexes.

Molecular dynamics (MD) simulations

MD simulations were used to produce a set of data at 200 ns using GROMACS. The interaction between graphyne AYC1 and AYT1 and the stability of complexes was investigated using MD simulations. The stability of the compound has been examined by analyzing RMSD and RMSF at a time interval of 200 ns [46]. As shown in Figure 5A, the amplitude of the RMSD curve changes indicates no major fluctuation in either Gy+AYC1 and Gy+AYT1 complexes in free graphyne. Which states that both the complexes are stable throughout the time [27]. The RMSD value for both Gy+AYC1 and Gy+AYT1 starts from zero and goes up to 3.2 nm and both complexes have higher RMSD values than graphyne, this might have happened due to the interaction formed between graphyne and aniline yellow derivatives.

Root-mean-square fluctuation (RMSF) measures to study parts of the structure that fluctuate, by calculating the average departure of a residue over time from its time-averaged position [47]. A greater variation in the RMSF value suggests a shift in the desired molecule's position, suggesting a higher probability of an interaction between the graphyne and aniline yellow derivatives [48]. Figure 5B shows that the values of RMSF are same for both Gy+AYC1 and Gy+AYT1 and both are strongly enhanced from graphyne [49]. Very high fluctuations are observed first after 40 atoms and secondly, after 90 atoms for both complexes

which indicates that AYC1 and AYT1 interact with graphyne. A high RMSF value means that during the simulation, the associated atoms are quite mobile and fluctuate a lot [50-55].

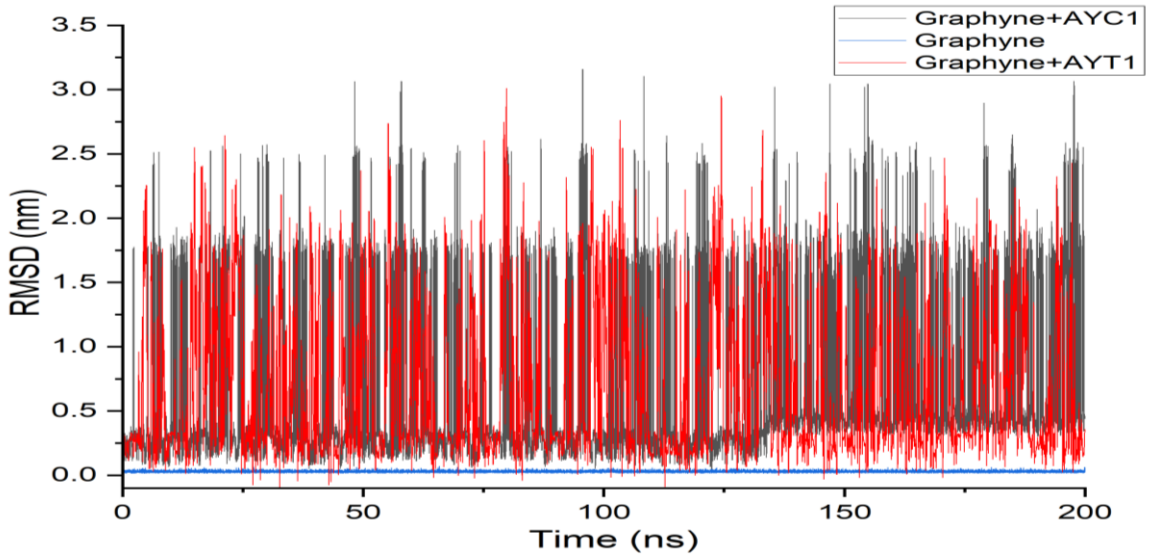

A

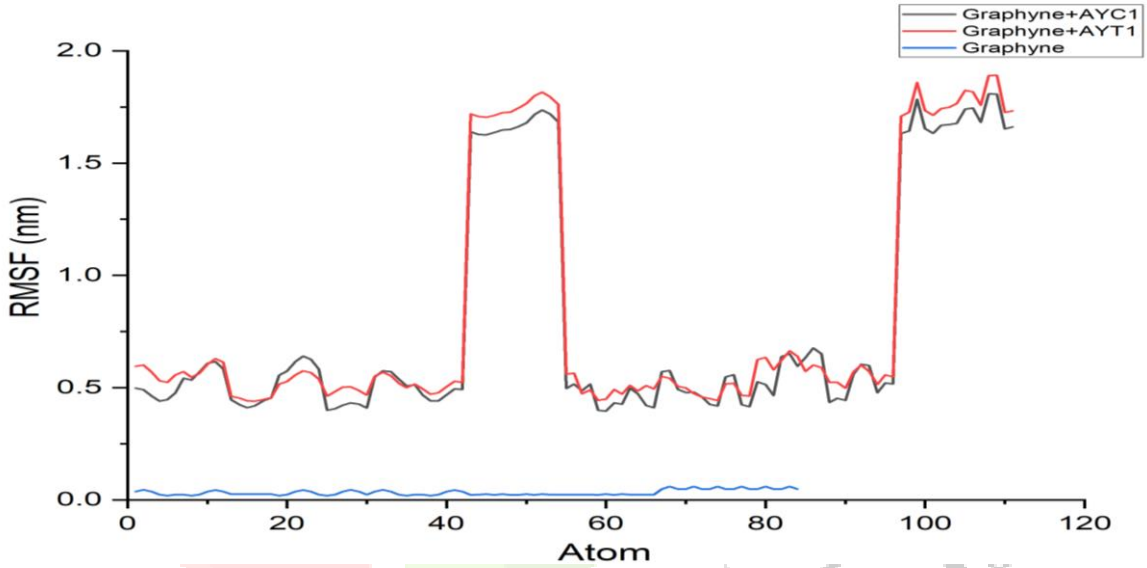

B

Figure 5: Plots of A) RMSD plots of graphyne, Gy+AYC1, and Gy+AYT1 complexes and B) RMSF plots of graphyne, Gy+AYC1, and Gy+AYT1 complexes.

Conclusion

The comprehensive study delves into the photochromic behavior of aniline yellow dye and its derivatives, emphasizing the significant energy differences between cis and trans isomers. AYC1/AYT1 derivatives display maximum change, with lower E_{HOMO}-E_{LUMO} gaps indicating heightened reactivity, and conductivity, and have better potential for electron donation nonlinear properties suggesting effective photoswitching capabilities. UV spectra analysis employing TD-DFT illustrates shifts in absorption band intensity during isomerization, indicating diverse photochemical behavior. Further exploration of AYC1 and AYT1 derivatives with graphyne reveals enhanced reactivity and conductivity, reduced E_{HOMO}-E_{LUMO} gaps, and stable interactions. The density of state (DOS) was performed which suggested a greater probability of charge transfer, which is also observed in the E_{HOMO}-E_{LUMO} gap by DFT calculation. GROMACS-based MD simulations confirm the stability of Gy+AYC1 and Gy+AYT1 complexes, offering

insights into their structural dynamics for potential applications in molecular interactions and materials science. The research concludes that these derivatives have the potential and might be used as photoswitching molecules.

Declarations

Ethical Approval: Not Applicable

Competing interests: We, the Corresponding authors) on behalf of all authors declare that this manuscript is original, has not been published before, and is not currently being considered for publication elsewhere. I further confirm that the order of authors listed in the manuscript has been approved by all of us. There is also no conflict of interest in any way.

Funding: Not Applicable

Availability of data and materials: Data will be made applicable on the request of reader.

Acknowledgement: Authors are thankful to Professor B. Jayaram for utilizing the facilities of SCFBio, Indian Institute of Technology, Delhi, India.

References

1. Coelho PJ, Castro MCR, Raposo MMM (2013) Reversible trans–cis photoisomerization of new pyrrolidene heterocyclic imines. J Photochem Photobiol A Chem 259:59–65. https://doi.org/10.1016/j.jphotochem.2013.03.004
2. Khayer K, Haque T (2020) Density Functional Theory Calculation on the Structural, Electronic, and Optical Properties of Fluorene-Based Azo Compounds. ACS Omega 5:4507–4531. https://doi.org/10.1021/acsomega.9b03839
3. Pirone D, Bandeira NAG, Tylkowski B, et al (2020) Contrasting Photo-Switching Rates in Azobenzene Derivatives: How the Nature of the Substituent Plays a Role. Polymers (Basel) 12:1019. https://doi.org/10.3390/polym12051019
4. F. Schedin, A. K. Geim, S. V. Morozov, E. W. Hill, P. Blake, M. I. Katsnelson and K. S. Novoselov, Nat. Mater., 2007, 6, 652.
5. F.-G. Ba˘nica˘, Chemical Sensors and Biosensors, John Wiley & Sons, Ltd, 2012.
6. J. Janata and A. Bezegh, Anal. Chem., 1988, 60, 62R.
7. K. Sinha Roy, D. R. Goud, A. Mazumder, B. Chandra, A. K. Purohit, M. Palit and D. K. Dubey, ACS Appl. Mater. Interfaces, 2019, 11, 16027.
8. N. Negreira, M. Lopez de Alda and D. Barcelo, J. Chromatogr. A, 2013, 1280, 64.
9. J. Zhang and Z. Chen, J. Chromatogr. A, 2017, 1530, 1. 27 D. W. Breck, Zeolite molecular sieves: structure, chemistry, and use, Wiley, 1973.
10. H. Shirakawa, E. J. Louis, A. G. MacDiarmid, C. K. Chiang and A. J. Heeger, J. Chem. Soc., Chem. Commun., 1977, 578, DOI: 10.1039/c39770000578.

11. K. S. Novoselov, A. K. Geim, S. V. Morozov, D. Jiang, Y. Zhang, S. V. Dubonos, I. V. Grigorieva and A. A. Firsov, Science, 2004, 306, 666.
12. B. F. Hoskins and R. Robson, J. Am. Chem. Soc., 1990, 112, 1546.
13. Merino E, Ribagorda M (2012) Control over molecular motion using the cis – trans photoisomerization of the azo group. Beilstein Journal of Organic Chemistry 8:1071–1090. https://doi.org/10.3762/bjoc.8.119
14. Gindre D, Boeglin A, Fort A, et al (2006) Rewritable optical data storage in azobenzene copolymers. Opt Express 14:9896. https://doi.org/10.1364/OE.14.009896
15. Dong L, Feng Y, Wang L, Feng W (2018) Azobenzene-based solar thermal fuels: design, properties, and applications. Chem Soc Rev 47:7339–7368. https://doi.org/10.1039/C8CS00470F
16. Calbo J, Thawani AR, Gibson RSL, et al (2019) A combinatorial approach to improving the performance of azoarene photoswitches. Beilstein Journal of Organic Chemistry 15:2753–2764. https://doi.org/10.3762/bjoc.15.266
17. Georgiev A, Kostadinov A, Ivanov D, et al (2018) Synthesis, spectroscopic and TD-DFT quantum mechanical study of azo-azomethine dyes. A laser induced trans-cis-trans photoisomerization cycle. Spectrochim Acta A Mol Biomol Spectrosc 192:263–274. https://doi.org/10.1016/j.saa.2017.11.016
18. Zhang X, Hou L, Samorì P (2016) Coupling carbon nanomaterials with photochromic molecules for the generation of optically responsive materials. Nat Commun 7:11118. https://doi.org/10.1038/ncomms11118
19. James A, John C, Owais C, et al (2018) Graphynes: indispensable nanoporous architectures in carbon flatland. RSC Adv 8:22998–23018. https://doi.org/10.1039/C8RA03715A
20. Chandra Shekar S, Swathi RS (2018) Molecular switching on graphyne and graphdiyne: Realizing functional carbon networks in synergy with graphene. Carbon N Y 126:489–499. https://doi.org/10.1016/j.carbon.2017.10.049
21. Rashid MAM, Hayati D, Kwak K, Hong J (2020) Theoretical Investigation of Azobenzene-Based Photochromic Dyes for Dye-Sensitized Solar Cells. Nanomaterials 10:914. https://doi.org/10.3390/nano10050914
22. IRMUMINOVA S, SEZGİN B, TİLKİ T (2020) Novel Heterocyclic Azo Compounds: Synthesis, Characterization and DFT Calculations. Süleyman Demirel Üniversitesi Fen Edebiyat Fakültesi Fen Dergisi 15:319–329. https://doi.org/10.29233/sdufeffd.820455
23. Georgiev A, Stoilova A, Dimov D, et al (2019) Synthesis and photochromic properties of some N-phthalimide azo-azomethine dyes. A DFT quantum mechanical calculations on imine-enamine tautomerism and trans-cis photoisomerization. Spectrochim Acta A Mol Biomol Spectrosc 210:230–244. https://doi.org/10.1016/j.saa.2018.11.033
24. Iijima, S. Helical microtubules of graphitic carbon. Nature 1991, 354, 56–58, doi:10.1038/354056a0.

25. Novoselov, K.S.; Geim, A.K.; Morozov, S.V.; Jiang, D.; Zhang, Y.; Dubonos, S.V.; Grigorieva, I.V.; Firsov, A.A. Electric Field Effect in Atomically Thin Carbon Films. Science 2004, 306, 666–669, doi:10.1126/science.1102896.
26. Ugarte, D. Onion-like graphitic particles. Carbon N. Y. 1995, 33, 989–993, doi:10.1016/0008-6223(95)00027-B.
27. Generalic, E. - "Allotrope." Croatian-English Chemistry Dictionary & Glossary, https://glossary.periodni.com (accessed on 30 December 2020)
28. Available online: https://www.cheaptubes.com (Accessed on 30 December 2020).
29. Konios, D.; Stylianakis, M.M.; Stratakis, E.; Kymakis, E. Dispersion behaviour of graphene oxide and reduced graphene oxide. J. Colloid Interface Sci. 2014, 430, 108–112, doi:10.1016/j.jcis.2014.05.033.
30. Li, H.; Song, S.I.; Song, G.Y.; Kim, I.I. Non-covalently functionalized carbon nanostructures for synthesizing carbon-based hybrid nanomaterials. J. Nanosci. Nanotechnol. 2014, 4, 1425–1440, doi:10.1166/jnn.2014.9048.
31. Li, T.F.; Xu, Y.H.; Li, K.; Wang, C.; Liu, X.; Yue, Y.; Chen, Z.; Yuan, S.J.; Wen, Y.; Zhang, Q.; et al. Doxorubicin-polyglycerol- nanodiamond composites stimulate glioblastoma cell immunogenicity through activation of autophagy. Acta Biomater. 2019, 86, 381–384, doi:10.1016/j.actbio.2019.01.020.
32. Zhang, Q.; Wu, Z.; Li, N.; Pu, Y.; Wang, B.; Zhang, T.; Tao, J. Advanced review of graphene-based nanomaterials in drug delivery systems: Synthesis, modification, toxicity and application. Mater. Sci. Eng. C 2017, 77, 1363–1377, doi:10.1016/j.msec.2017.03.196.
33. Bujak K, Wasiak A, Sobolewska A, et al (2020) A family of azoquinoline derivatives: Effect of the substituent at azo linkage on thermal cis-trans isomerization based on an experimental and computational approach. Dyes and Pigments 175:108151. https://doi.org/10.1016/j.dyepig.2019.108151
34. Piyanzina I, Minisini B, Tayurskii D, Bardeau J-F (2015) Density functional theory calculations on azobenzene derivatives: a comparative study of functional group effect. J Mol Model 21:34. https://doi.org/10.1007/s00894-014-2540-x
35. Duan R, Wu D, Tang L, et al (2020) Interactions of the cis and trans states of an azobenzene photoswitch with lysozyme induced by red and blue light. Spectrochim Acta A Mol Biomol Spectrosc 229:117965. https://doi.org/10.1016/j.saa.2019.117965
36. Solomon RV, Veerapandian P, Vedha SA, Venuvanalingam P (2012) Tuning Nonlinear Optical and Optoelectronic Properties of Vinyl Coupled Triazene Chromophores: A Density Functional Theory and Time-Dependent Density Functional Theory Investigation. J Phys Chem A 116:4667–4677. https://doi.org/10.1021/jp302276w
37. Ye Z, Xie S, Cao Z, et al (2021) High-rate aqueous zinc-organic battery achieved by lowering HOMO/LUMO of organic cathode. Energy Storage Mater 37:378–386. https://doi.org/10.1016/j.ensm.2021.02.022

38. Majumdar D, Lee HM, Kim J, et al (1999) Photoswitch and nonlinear optical switch: Theoretical studies on 1,2- bis -(3-thienyl)-ethene derivatives. J Chem Phys 111:5866–5872. https://doi.org/10.1063/1.479881
39. Seferoğlu N, Toprakçıoğlu G (2019) Detailed theoretical characterization of azo chromophores containing dicyanomethylene acceptor and various coupling components by DFT. J Mol Struct 1181:360–372. https://doi.org/10.1016/j.molstruc.2018.12.080
40. Kathan M, Hecht S (2017) Photoswitchable molecules as key ingredients to drive systems away from the global thermodynamic minimum. Chem Soc Rev 46:5536–5550. https://doi.org/10.1039/C7CS00112F
41. Solomon RV, Jagadeesan R, Vedha SA, Venuvanalingam P (2014) A DFT/TDDFT modelling of bithiophene azo chromophores for optoelectronic applications. Dyes and Pigments 100:261–268. https://doi.org/10.1016/j.dyepig.2013.09.016
42. Martynov AG, Mack J, May AK, et al (2019) Methodological Survey of Simplified TD-DFT Methods for Fast and Accurate Interpretation of UV–Vis–NIR Spectra of Phthalocyanines. ACS Omega 4:7265–7284. https://doi.org/10.1021/acsomega.8b03500
43. Bujak K, Orlikowska H, Małecki JG, et al (2019) Fast dark cis-trans isomerization of azopyridine derivatives in comparison to their azobenzene analogues: Experimental and computational study. Dyes and Pigments 160:654–662. https://doi.org/10.1016/j.dyepig.2018.09.006
44. Rashid MAM, Hayati D, Kwak K, Hong J (2020) Theoretical Investigation of Azobenzene-Based Photochromic Dyes for Dye-Sensitized Solar Cells. Nanomaterials 10:914. https://doi.org/10.3390/nano10050914
45. Rashid MAM, Hayati D, Kwak K, Hong J (2020) Theoretical Investigation of Azobenzene-Based Photochromic Dyes for Dye-Sensitized Solar Cells. Nanomaterials 10:914. https://doi.org/10.3390/nano10050914
46. Goodarzi, S.; Da Ros, T.; Conde, J.; Sefat, F.; Mozafari, M. Fullerene: Biomedical engineers get to revisit an old friend. Mater. Today 2017, 20, 460–480, doi:10.1016/j.mattod.2017.03.017.
47. Rehman, A.; Houshyar, S.; Wang, X. Nanodiamond in composite: Biomedical application. J. Biomed. Mater. Res. Part A 2020, 108, 906–922, doi:10.1002/jbm.a.36868.
48. Ahlawat, J.; Masoudi Asil, S.; Guillama Barroso, G.; Nurunnabi, M.; Narayan, M. Application of carbon nano onions in the biomedical field: Recent advances and challenges. Biomater. Sci. 2021, doi:10.1039/d0bm01476a.
49. Kushwaha, S.K.S.; Ghoshal, S.; Rai, A.K.; Singh, S. Carbon nanotubes as a novel drug delivery system for anticancer therapy: A review. Braz. J. Pharm. Sci. 2013, 49, 629–643, doi:10.1590/S1984-82502013000400002.
50. Ferrari, M. BioMEMS and biomedical nanotechnology. In BioMEMS and Biomedical Nanotechnology; Springer: Berlin/Heidelberg, Germany, 2007; pp. 2–17, ISBN 0387255664.
51. Tsang, S.C.; Chen, Y.K.; Harris, P.J.F.; Green, M.L.H. A simple chemical method of opening and filling carbon nanotubes. Nature 1994, 372, 159–162, doi:10.1038/372159a0.

52. Ajayan, P.M.; Ebbesen, T.W.; Ichihashi, T.; Iijima, S.; Tanigaki, K.; Hiura, H. Opening carbon nanotubes with oxygen and implications for filling. Nature 1993, 362, 522–525, doi:10.1038/362522a0.
53. Ebbesen, T.W. Wetting, filling and decorating carbon nanotubes. J. Phys. Chem. Solids 1996, 57, 951–955, doi:10.1016/0022- 3697(95)00381-9.
54. Rastädter D, Biswas M, Burghardt I (2014) Molecular Dynamics Study of the Controlled Destabilization of an RNA Hairpin Structure by a Covalently Attached Azobenzene Switch. J Phys Chem B 118:8478–8488. https://doi.org/10.1021/jp501399k
55. Martínez L (2015) Automatic Identification of Mobile and Rigid Substructures in Molecular Dynamics Simulations and Fractional Structural Fluctuation Analysis. PLoS One 10:e0119264. https://doi.org/10.1371/journal.pone.0119264